Numerical Analysis of Plasmonic Couplers based on Metallic Lens

Cosme E. Rubio-Mercedes[1] , Nilson H. O. Cunha[2] , José P. da Silva[2]
[1]Mathematics and Engineering Physics Programs, Mato Grosso do Sul State University (UEMS), Dourados–MS, Brazil. cosme@uems.br
[2]Post Graduate Program in Electrical and Computer Engineering, Federal University of Rio Grande do Norte (UFRN), Natal–RN, Brazil. nilson.ee@gmail.com and jose.patrocinio@ufrn.br.

Abstract— **Surface Plasmon Polaritons (SPPs) are evanescent surface electromagnetic waves that propagate along a dielectric-metal interface. They allow propagating modes in waveguides with dimensions smaller than the diffraction limit. By arranging slits of different widths along a metallic film, it is possible to design plasmonic lenses through phase modulation at the slits output. The distance of energy concentration, obtained by these lenses, its called focus and is of the order of one wavelength (λ). Lenses of this type allow light coming from a micrometric waveguide, such as optical fibers, for example, to be coupled to structures such as nanometric waveguides, at short distances, reducing considerably the coupling area. In this work, by using the Finite Element Method (FEM) was simulated the energy coupling between a light source and a plasmonic waveguide using plasmonic lens operating at wavelengths of 650 nm.**

Index Terms— Finite elements, Optical coupler, Plasmonic lens, Plasmonic waveguides.

I. INTRODUCTION

The transmission of light through sub wavelength metallic apertures with low losses brought up a new era for the design of new types of nanophotonic circuits [1]-[9]. It makes possible to design several devices such as bends, couplers, nano waveguides and lenses.

Plasmonic is the science that studies the behaviour of plasmons. When light interacts at an interface composed by a dielectric material with another conductive material, dense waves of electrons are formed on this surface, and these waves are called plasmons [10]. When this energy accumulated at the metallic interface comes into contact with a non-conductor material, particles called polaritons are formed, hence the term Surface Plasmon Polaritons (SPP) to refer to these surface waves at high frequencies [11], [12].

In this context, the study of plasmonic allowed the optical industry to absorb this technology, giving rise to a new range of devices and applications. An example of this is the plasmonic lenses, which are devices that permit subwavelength focusing of light in the visible spectra and in the near infrared (NIR) [1]-[3]. At optical frequencies, these structures can be implemented by alternating nanocapacitors and nanoinductors which can be obtained by using dielectric and plasmonic structures, respectively [4]-[6].

Optical lenses are excellent candidates for coupling light between two optical devices such as sources and dielectric or plasmonic waveguides. Like conventional lenses, plasmonic lenses have the objective

of receiving an excitation and creating a focal point at the output. However, with the advancement of technology, it is increasingly necessary for devices to present a high performance, and it is at this point that conventional lenses begin to decay, since their focal point is defined by the curvature in the geometry, and as frequencies increase the geometry of these devices tends to be smaller and smaller, which can make them unfeasible [13].

To solve this problem, lenses composed with metamaterials [14], [15] were proposed, which defined the focal point based on the unit cells that would compose the structure, that is, the focus is independent of the curvature of the lens, but this technology presents some complexity in its prototyping. In this way, plasmonic lenses can be used as an alternative to solve these problems, since, like metamaterial lenses, plasmonic lenses are independent of the lens geometry, since the focal point will be created based on the aperture formed by the plasmonic materials but presenting a simpler and much more practical construction process for current prototyping standards.

Due to the characteristics of the applications, the metals used to build a plasmonic structure need to be noble metals, as these can support surface plasmons. Noble metals are particularly effective in plasmonic because their valence electrons are highly mobile, making them able to interact strongly with light, in addition to being highly resistant to oxidation and corrosion [16], [17]. In this way, silver (Ag), gold (Au) and copper (Cu) are the most prominent materials that can be used for plasmonic lenses fabrication due to its relatively easy acquisition.

Since metals are very dispersive materials which exhibit different values of complex refractive index, depending on the operating wavelength, the lens characteristics, such its chromatic aberration and full width at half maximum (FWHM) should be analysed for polychromatic illumination operation [18].

In this context, this work will design and analyse silver plasmonic lenses, with dielectric permittivity (ε) values obtained from [1] and [7], varying the lens configuration parameters [8], and their use as a compact coupler between an external light source and a plasmonic waveguide.

In section II of this work the design of the plasmonic lenses used will be presented. Section III will discuss the simulations carried out, presenting the results obtained and the discussions relevant to each topic, and finally in Section IV the conclusions obtained in this study will be presented.

II. PLASMONIC LENS PROJECT

In an optical circuit, in which a source provides energy to be transported in a waveguide, it is essential to use coupling devices that will increase the system efficiency, reducing possible dispersion losses at the coupling point.

In this context, Fig. 1 shows the setup proposed in this work, in which the coupling will be performed by means of a plasmonic lens.
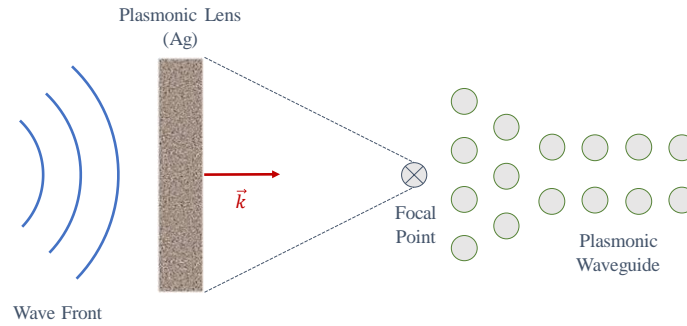
Fig. 1. Schematic of Ag plasmonic coupler, adapted from [9].

First, a study was carried out on the focal point of light by using a nano-slit lens or also called near-field focusing plate [1], [3], [6]. An already developed computational model [19], [20] was used to simulate a silver (Ag) lens, see Fig. 2, with the same dimensions described in [1]. This structure focuses the light in the transversal direction because of its two-dimensional (2D) nature. The parameters lens are the diameter of the lens aperture $D = 4\ \mu m$, the thickness of the Ag film $d = 500\ nm$ and the minimum spacing between slits $e = 40\ nm$.
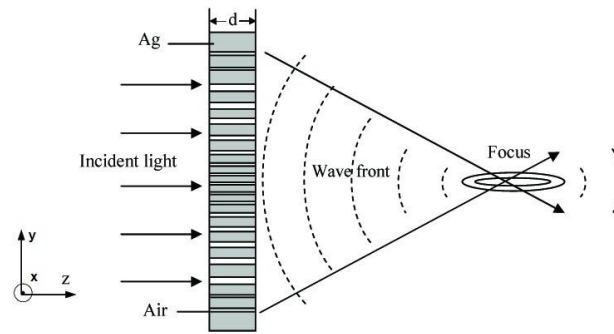
Fig. 2. Schematic of a nano-slit array with different width formed on thin metallic film. Metal thickness is d, and each slit width is determined for required phase distribution on the exit side, respectively. A TM-polarized plane wave is incident to the slit array from the left side. Reprinted with permission from [1].

The lens is designed to operate at a wavelength of $\lambda = 650\ nm$, and with a focal length of $f = 600\ nm$. The relative permittivity used for the silver at this wavelength is $\varepsilon_r = -16.6338 + j0.5$ [7]. As noted in [1], the minimum spacing between slits e must be greater than $24\ nm$, which is the value of the silver penetration constant at $\lambda = 650\ nm$.

III. METHOD OF ANALYSIS

According to [19] and [20], it was considered a general bidimensional structure (2D) as shown in Fig. 2, where the computational domain is on the plane $y - z$ and there is no variation along the x axis ($d/dx = 0$). PMLs are used to simulate an open boundary and avoid reflections from the computational window. The 2D scalar equation, in frequency domain, governing the transverse electric (TE) and the transverse magnetic (TM) fields on the plane $y - z$ is written as:

$$s_y \frac{\partial}{\partial y}\left(p \frac{s_y}{s} \frac{\partial \varphi}{\partial y}\right) + s_z \frac{\partial}{\partial z}\left(p \frac{s_z}{s} \frac{\partial \varphi}{\partial z}\right) + k_0^2 q s \varphi = 0 \; ; \tag{1}$$

where

$$\varphi = E_z \, , p = 1 \, , q = n^2 \, , \text{for TE modes} \; ; \tag{2}$$

and

$$\varphi = H_z \, , p = 1/n^2 \, , q = 1 \, , \text{for TM modes ;} \qquad (3)$$

where $k_0 = 2\pi/\lambda_0$, λ_0 is the free space wavelength. E_z and H_z are the z components of the electric and magnetic fields, respectively, n is the refractive index, defined in [19] and [20]. The s and s_i ($i = x, y, z$) are the PML parameters, and they can be determined as follows:

$$s_i = 1 - j \left(\frac{\rho}{d_i}\right)^2 \tan (\delta_i) \qquad (4)$$

where ρ is the distance from the beginning of PML, d_i is the PML thickness, and δ_i is the angle at the end of PML ($\rho = d_i$) [20]. The PML was ideally designed, that is, every wave incident on its surface will be absorbed. In other words, the estimated total reflection level was zero.

For the numerical analysis of the structure, the Galerkin formulation is applied to solve (1), which is called the bidimensional Finite Elements Method (2D-FEM). In this formulation, the x and y coordinates represent the transverse directions and z represents the propagation direction, as shown in Fig. 2. For the entire structure, including the PML, a single mesh was considered, as the algorithm identifies the regions of the structure based on the defined materials.

IV. RESULTS AND DISCUSSIONS

Initially, the computational domain considered was of $-1.20 \, \mu m \leq z \leq 3.15 \, \mu m$ and $-2.20 \, \mu m \leq y \leq 2.2 \, \mu m$ divided in 64,059 triangular elements of quadratic order (128,890 points), where the PMLs are the outer layers of $0.2 \, \mu m$ and $0.5 \, \mu m$ in y and z coordinates, respectively. The incident field is a TM-polarized plane wave and is placed at $z = -0.65 \, \mu m$. The near-field focusing structure starts at $z = -d \, nm$ and ends at $z = 0$. The field intensity distribution for the lens designed to operate at $\lambda = 650 \, nm$ is shown in Fig. 3. The lens has 66 slits and the slit widths were obtained from the interpolation of the function that models the slit width in relation to the central position of the lens [1].
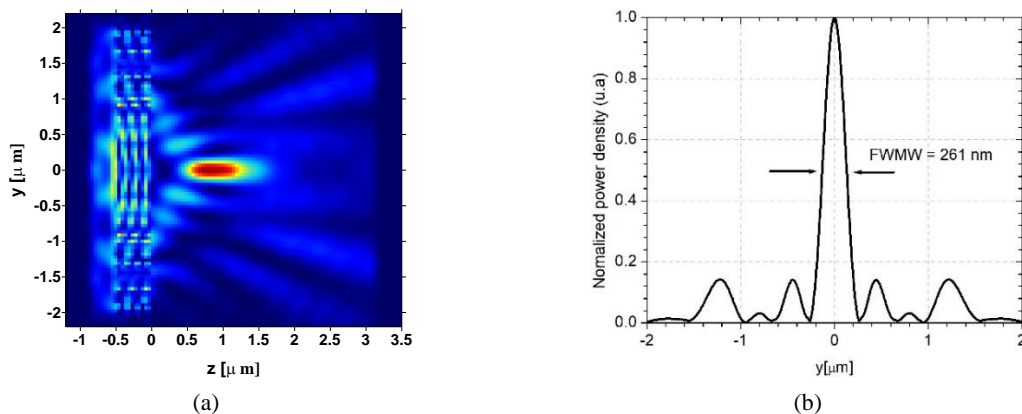

(a)   (b)

Fig. 3. *(a)* Magnetic field distribution, and *(b)* Transversal intensity profile at Zmax = 765 nm.

From Fig. 3, it can be seen that the simulated lens has a $FWHM = 261 \, nm$ with a depth of focus (DOF) of $781 \, nm$. Note that the maximum focus point, $Z_{max} = 736 \, nm$, does not match the projected focal length $f = 600 \, nm$. However, the lens design equations are based on geometric optics, which, despite being extremely useful, are not strictly accurate in the near-field region and the projected focal

length is within the half-power focal length [8]. The results obtained here are very consistent with the results presented in [1], showing that this plasmonic lens configuration can be used as a compact coupler.

In Fig. 4(a) it is shown the power density, along the horizontal line (z axis) at the center of the lenses ($y = 0$) for silver relative permittivity of $\varepsilon_{r1} = -16.6338 + j0.5$ (blue line) [7] and $\varepsilon_{r2} = -17.36 + j0.715$ (red line) [1]. The lens with permittivity ε_{r1} has DOF equal to $781\ nm$, while the lens with permittivity ε_{r2} has a DOF equal to $811\ nm$. The sudden energy variation within the lens region, which corresponds to the interval $-0.5\ \mu m \leq z \leq 0\ \mu m$, demonstrates two characteristics of SPPs: a large increase in field intensity within the lens and a change in the wavelength that propagates in the central slit. Both simulated lenses have a small maximum difference of only 5%. Thus, the lens with the permittivity value obtained from [7] has focus smaller than the lens focus with the permittivity obtained from [1], showing a favourable reduction of the focal length, which is desirable for the Z_{max} reduction. The bandwidth (BW) is defined as the range of wavelength where the power density at the maximum focus point is greater than a chosen threshold, for example 50% of the maximum peak of the density energy curve in function of wavelength [8]. In Fig. 4(b) are presented the BWs of the lens with silver permittivity ε_{r1}. The dashed horizontal lines represent the thresholds of 50%, 80% and 90% of the maximum peak power density, respectively. For a threshold of 50%, the lens has three BWs: from $424\ nm$ to $452\ nm$ ($BW = 28\ nm$); from $456\ nm$ to $469\ nm$ ($BW = 13\ nm$) and from $483.15\ nm$ to $730\ nm$ ($BW = 246.85\ nm$). For a threshold of 80% a BW region from $511\ nm$ to $619\ nm$ ($BW = 108\ nm$) is perceived and for a threshold of 90% there are three BWs: from $514\ nm$ to $523\ nm$ ($BW = 9\ nm$); $534\ nm$ to $542\ nm$ ($BW = 8\ nm$) and from $552\ nm$ to $602\ nm$ ($BW = 50\ nm$). It is also observed in Fig. 4(b) that the maximum power density, obtained at wavelength $\lambda = 586\ nm$, is not reached at the lens operating wavelength ($\lambda = 650\ nm$), it is expected because SPP excitation occurs for surface plasmons (SP) wavelength $\lambda_{SP} = 632\ nm$.
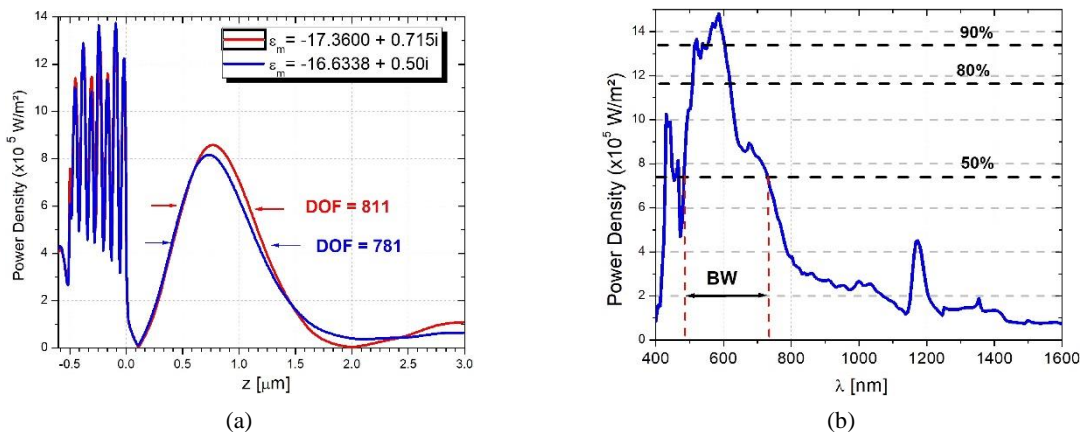

Fig. 4. (a) Power density in a horizontal line along the z axis at the center of the projected lens and (b) Power density at thepoint of maximum focus (Zmax) in function of wavelength, where the horizontal lines represent the 50%, 80%, and 90% thresholds of the curve's maximum value

A. Determination of the coupling lens

To determine the best lens to be used as plasmonic coupler, several lens configurations operating at the wavelength of $\lambda = 650\,nm$ and with a focus length of $f = 600\,nm$ were designed. A study was carried out on the robustness of the lens against possible variations of design parameters, such as the lens depth d and minimum spacing between slits e, as well as noting that there is the possibility of optimizing the coupling efficiency of the plasmonic lens in function of those parameters. The values of the d parameter was chosen as being $410\,nm$, $500\,nm$, $550\,nm$ and $610\,nm$. For each lens depth d value considered, the minimum spacing between slits, e, assumes the values $25\,nm$, $35\,nm$, $40\,nm$, $45\,nm$ and $55\,nm$, totalizing twenty lens variations.

In Figs. 5(a)-(d), is presented the power density (or Poynting vector), in a horizontal line in the middle of the lens ($y = 0$), for the lens depth values of $d = 410\,nm$, $d = 500\,nm$, $d = 550\,nm$, $d = 610\,nm$, respectively, where the spacing between slits are: $25\,nm$ (black line), $35\,nm$ (red line), $40\,nm$ (blue line), $45\,nm$ (magenta line), $55\,nm$ (green line). In general, the maximum focus position (Z_{max}) increases for small values of the minimum spacing between slits e.

(a) d = 410
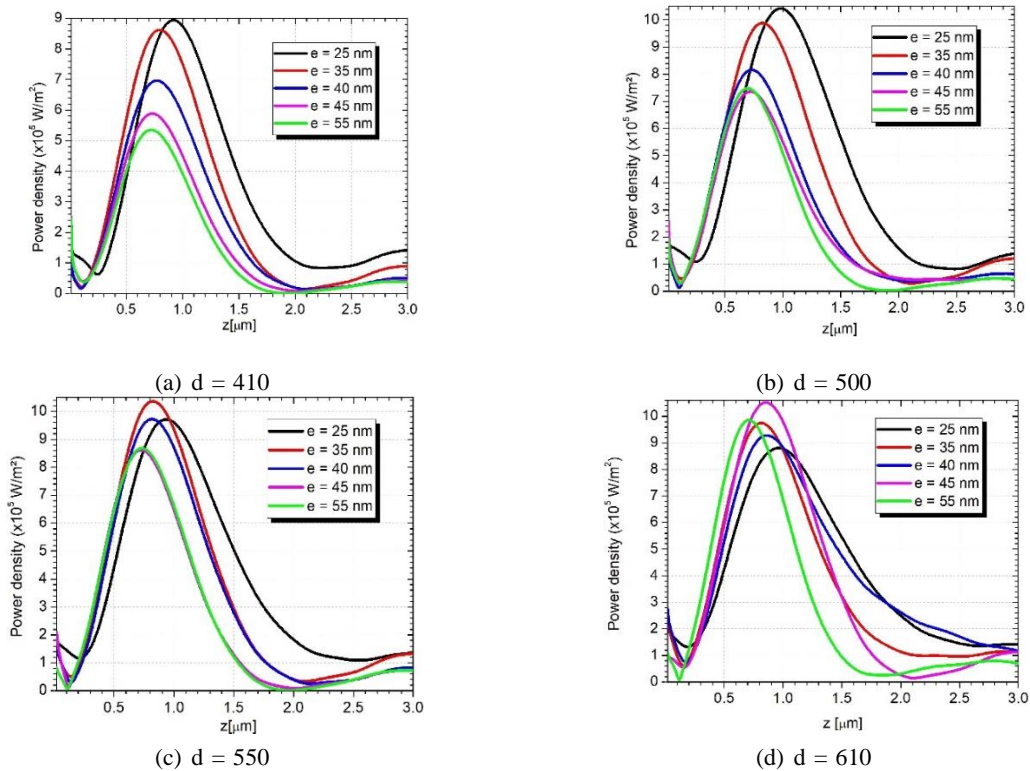
(b) d = 500

(c) d = 550

(d) d = 610

Fig. 5. Power density in the centre of the transversal domain (line y = 0) of lenses with thickness of the film of: (a) d = 410nm, (b) d = 500 nm, (c) d = 550 nm and (d) d = 610 nm. Five values of the spacing between slits **e** are considered: 25 nm (black line), 35 nm (red line), 40 nm (blue line), 45 nm (magenta line), 55 nm (green line).

From Figs. 5(a)-(b), it is possible to see that, in both lenses with $d = 410\,nm$ and $d = 500\,nm$, the curves that present the maximum power intensity are obtained for a minimum spacing between slits of $e = 25\,nm$. When comparing the maximum power densities of both the lenses, with $d = 410\,nm$ and $d = 500\,nm$, and with $e = 25\,nm$, it is noticed that the lens with $d = 410\,nm$ is approximately $e = 14\%$ smaller than the intensity of the lens with $d = 500\,nm$ and both lenses have Z_{max} equal to

$919\ nm$. Observing the Figs. 5(c)-(d), the lens with minimum spacing between slits of $e = 35\ nm$ and $d = 550\ nm$, in Fig. 5(c), and the lens with minimum spacing between slits e = 45 nm and $d = 610\ nm$, in Fig. 5(d), have maximum power density, being 0.58% smaller and 0.96% greater than that of maximum power density with $e = 25\ nm$ and $d = 500\ nm$ in Fig. 5(b), respectively. Both these lenses, $d = 550\ nm$ and $d = 610\ nm$, have maximum power density close to that lens with $e = 25\ nm$ and $d = 500\ nm$ of Fig. 5(b) and have focal lengths of $Z_{max} = 826\ nm$ and $Z_{max} = 856\ nm$, respectively. Therefore, the lens with $d = 550\ nm$ and $e = 35\ nm$ is the most suitable of the lenses analysed in this work, to perform the coupling in photonic structures at the nano-metric scale, as it has a focus length near to the projected one. This lens has a FWHM and DOF of $277\ nm\ (0.42\lambda)$ and $832\ nm$, respectively and will be defined as an optimal coupling lens in this work.

In Table I, are presented the Z_{max} values and maximum power density (S_z) for the thickness of the film $d = 500\ nm$ and the five values of the minimum spacing between slits e: $25\ nm$, $35\ nm$, $40\ nm$, $45\ nm$ and $55\ nm$. The lens with $e = 25\ nm$ has a maximum power density approximately 28% greater than the lens with $e = 40\ nm$ and a Z_{max} value of 983 nm, which is 247 nm greater than the maximum focus position of that lens.

TABLE I. MAXIMUM FOCUS POSITION (ZMAX) AND MAXIMUM POWER DENSITY FOR THE THICKNESS OF THE LENS D = 500 NM.

e	$Zmax\ [nm]$	$Sz \times 10^4\ [W/m^2]$
25	983	10.42
35	825	9.88
40	736	8.16
45	722	8.58
55	701	7.48

Next, since silver is a dispersive material, the calculation of Z_{max} and maximum $\vec{S}_z$ in function of wavelength was performed, for the optimal coupling lens ($e = 35\ nm$ and $d = 550\ nm$) obtained in this work, respectively, see Fig. 6.
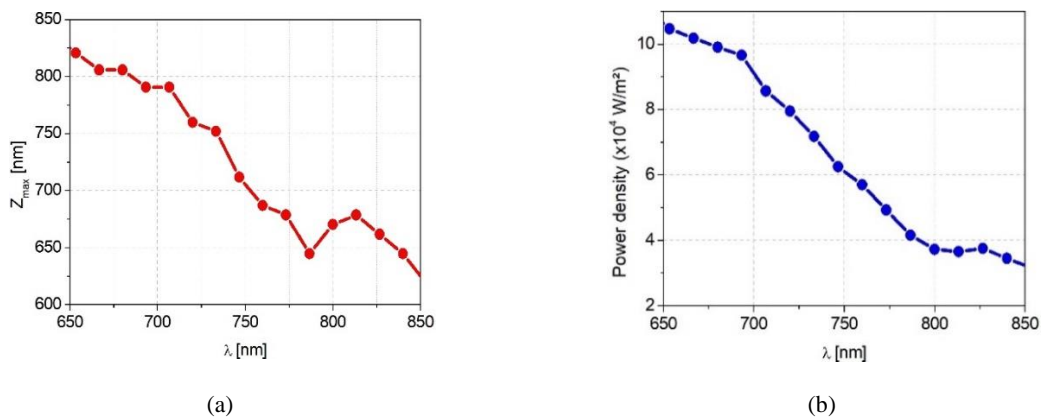

Fig. 6. (a) Position of the peak power intensity (Zmax) for the lens composed by silver designed to operate at the central wavelength of 650 nm and (b) power density at Zmax = 826 nm in function of wavelength.

In Fig. 6(a) is observed that Z_{max} decreases with the increase of the wavelength values. It approaches the projected focus value $f = 600\ nm$ at wavelengths region from 800 nm to 850 nm. Also, the power

density at $Z_{max} = 826\ nm$ decreases with the increase of the wavelength values, as can be seen in Fig. 6(b), which causes the lens coupling in waveguide structures to be restricted to certain ranges of the wavelengths.

B. Plasmonic lens coupling

In this section, an analyse will be carried out on the coupling of magnetic energy in to two types of plasmonic waveguides. The light is couple, from an external source/dielectric waveguide to a metallic-dielectric-metallic (MDM) plasmonic waveguide initially, and then to a plasmonic waveguide made of double chain of silver nanocylinders.

1) Coupling to an MDM plasmon waveguide

First, it was considered a coupler created by placing a plasmonic lens to couple energy from an external waveguide to a two-dimensional MDM plasmonic waveguide. Was used the optimized lens obtained in the previous section, which has lens depth $d = 550\ nm$ and $e = 35\ nm$. Fig. 7 shows the computational domain of the coupling lens and the MDM waveguide, where w_P is the MDM waveguide width and A is a parameter that is called coupling distance between the plasmonic lens and the MDM waveguide. The PMLs are the outer layers of $0.5\ \mu m$ in both coordinates in y and z directions. The structure was excited with a TM-polarized plane wave at the wavelength of $\lambda = 650\ nm$.
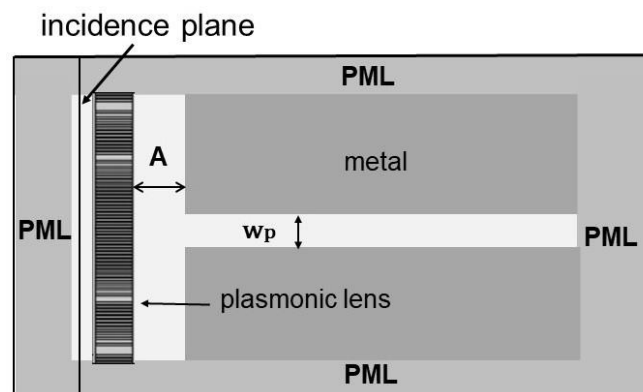

Fig. 7. Two-dimensional computational scheme for the 2D-FEM simulation of the magnetic waves in plasmonic couplers. The coupler, created by placing a coupling lens to couple energy from an external dielectric waveguide or fiber to an MDM plasmonic waveguide.

Simulations were made for coupling lenses in function of coupling distance A, with values in the range from $600\ nm$ to $850\ nm$, for various values of widths (w_P) of plasmonic waveguides. Fig. 8 shows the coupling efficiency and the reflection coefficient for various values of waveguide widths at the wavelength $\lambda = 650\ nm$.
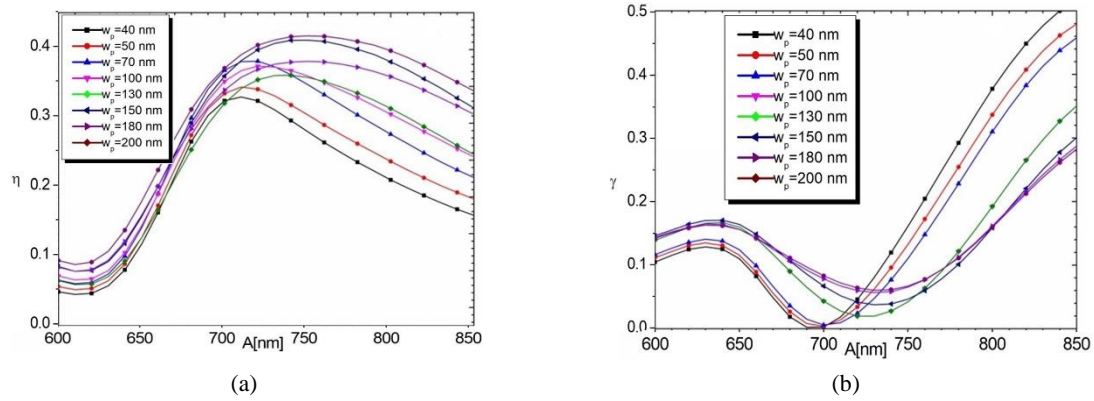
(a)   (b)

Fig. 8. Coupling efficiency (a) and reflection (b) for MDM plasmonic waveguides widths of w_p values: 40 nm (black line), 50 nm (red line), 70 nm (blue line), 100 nm (magenta line), 130 nm (green line), 150 nm (dark blue line), 180 nm (purple line) and 200 nm (brown line) at the wavelength $\lambda = 650$ nm in function of the coupling distance A.

For the MDM waveguides analysed, coupling distances A at which maximum coupling coefficients are in the value range between the design focal length ($600\ nm$) and the maximum focal length Z_{max} ($826\ nm$). The best coupling efficiency is obtained for the MDM waveguide of width $w_P = 150\ nm$ and $w_P = 200\ nm$ located at a coupling distance of $A = 750\ nm$. However, it is not at this position that the minimum reflection occurs as seen in Fig. 8(b). The minimum reflection for the waveguide width $w_P = 200\ nm$ is obtained for a coupling distance $A = 730\ nm$ with a reflection of 0.067. It is observed that the maximum focal length Z_{max} of the plasmonic lens is not always the distance that provides the best coupling in the MDM waveguide.

In Fig. 9 is calculated the coupling efficiency and the reflection in function of the width w_P of the MDM waveguide for various coupling distances values A.
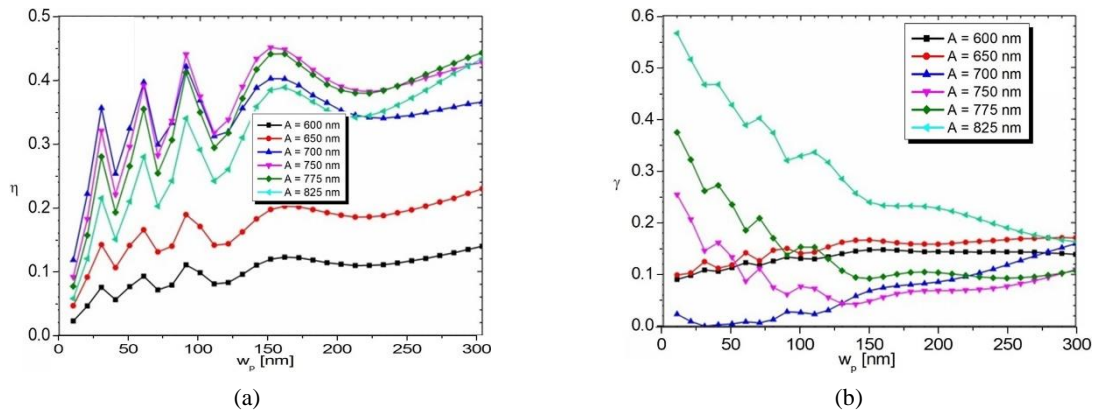

(a)   (b)

Fig. 9. Coupling efficiency (a) and reflection (b) in function of the MDM waveguide width wp for different coupling distance A, namely 600 nm (black line), 650 nm (red line), 700 nm (blue line), 750 nm (magenta line), 775 nm (green line) and 825 nm (light blue).

In Fig. 9(a) it is possible to verify again that the coupling distance at which the best coupling occurs is $A = 750\ nm$. The reflection coefficient is also calculated, see Fig. 9(b), where the coupling distance that has the minimum reflection is $A = 750\ nm$ with $w_P = 150\ nm$.

Waveguides with small w_P have high coupling efficiency as can be seen in Fig. 9(a) where waveguide widths of $30\ nm$, $60\ nm$, $90\ nm$ and $150\ nm$ with a distance of $A = 750\ nm$ (magenta line) have the highest coupling efficiency peaks corresponding to 0.32, 0.39, 0.44 and 0.45 values, respectively, all

these simulation having reflection below of 0.2. Note that waveguides with widths w_P close to the focal width ($FWHM = 277\ nm$) have a good coupling efficiency, however, they must have evanescent modes because their reflection value is relatively high. In Fig. 9(b) the small waveguides widths w_P show large reflections coefficient, having about 0.56 value, for $A = 825\ nm$ and for waveguides width w_P equal to $10\ nm$, confirming again that the Z_{max} of the coupling lens does not provide the best coupling efficiency.

In Figs. 10(a)-(f) the behaviour of the magnetic field $|H_z|$ was simulated to demonstrate the coupling to the MDM plasmonic waveguide for different widths of w_P: (a) $30\ nm$, (b) $60\ nm$, (c) $90\ nm$, (d) $150\ nm$, (e) $200\ nm$ and (f) $277\ nm$ by using a coupling distance of $A = 750\ nm$ in the plasmonic lens.
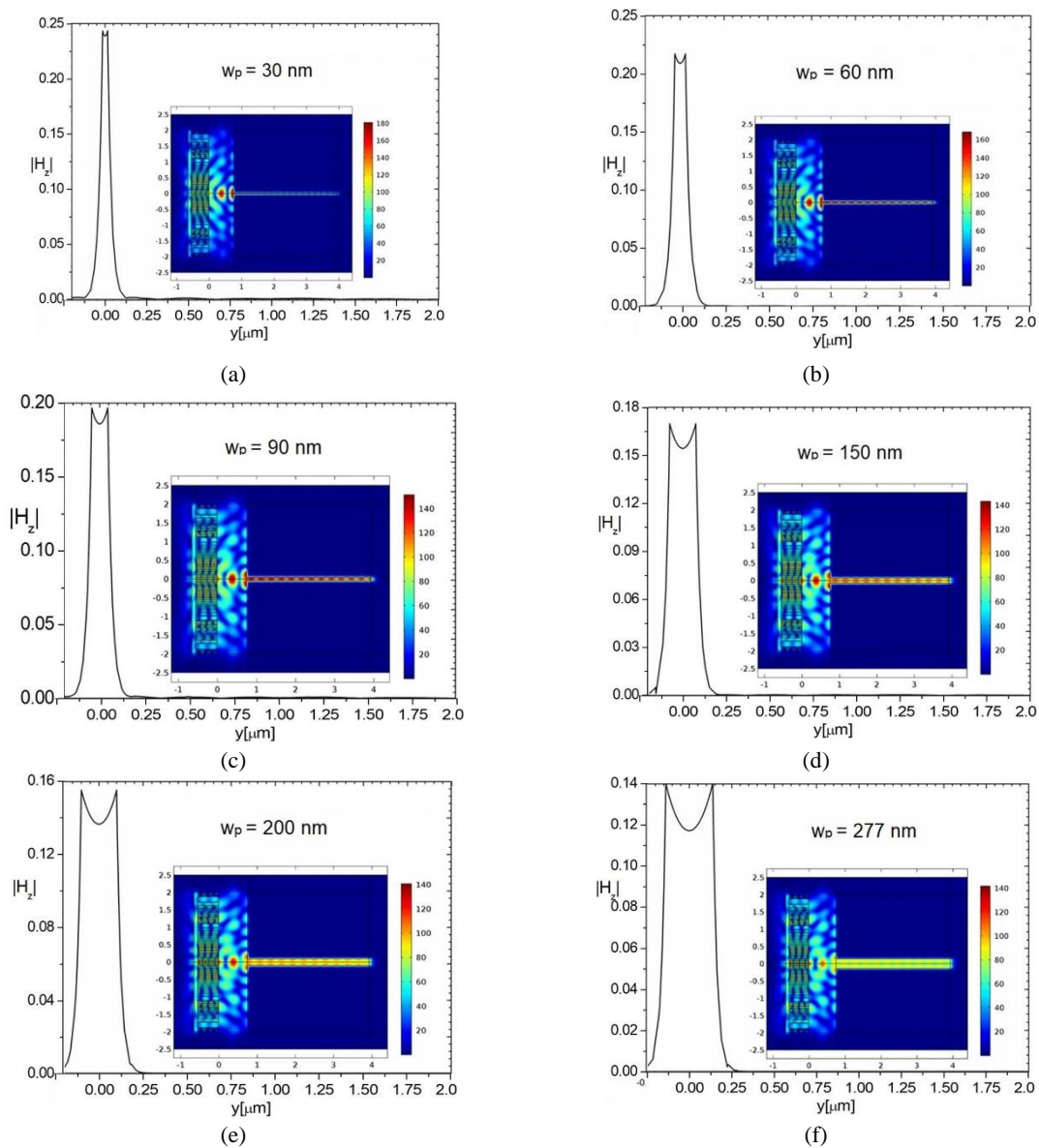

Fig. 10. Coupling magnetic fields for the MDM waveguides with widths of w_P: (a) 30 nm, (b) 60 nm, (c) 90 nm, (d) 150 nm, (e) 200 nm and (e) 277 nm with coupling distance A equal to 750 nm in the plasmonic lens.

Based on results obtained in Fig. 10, it is verified that the magnetic field decreases by increasing the

waveguide width, and despite this, the energy coupled to large-width waveguides is still high. This demonstrates that the best couplings it is not obtained only in MDM waveguides that have a width comparable to the FWHM of the plasmonic lens. From the results of this simulation, it can see that the plasmonic lens has great coupling capabilities to couple energy from an external waveguide to an MDM waveguide. The results show that there is a coupling efficiency approximately up to 50%, and having efficiency characteristics that allow coupling to small width waveguides located at coupling distance close to the Z_{max}.

2) Coupling to plasmon waveguide based on double chain of metal cylinders.

To couple energy from a source to a plasmonic waveguide, a 2D plasmon waveguide made of double chain of silver nanocylinders [9] and the studied plasmonic lens were used. In Fig. 11, it is shown the schematic of the coupler lens and the coupling of the light beam to the plasmonic waveguide is made from the left to the right. Here, the computational domain was of $-2.7\ \mu m \leq z \leq 15.3414\ \mu m$ and $-2.5\ \mu m \leq y \leq 2.5\ \mu m$ divided in 72,245 elements (145,726 points), where the PMLs are the outer layers of $0.5\ \mu m$ and $2.0\ \mu m$ in y and z coordinates, respectively.
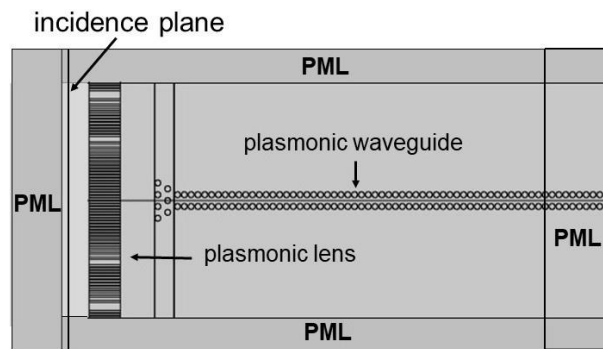

Fig. 11. Two-dimensional computational scheme for the FEM simulation of the EM waves in plasmonic couplers. The coupler, created by placing a plasmonic lens to couple energy from an external dielectric source to a plasmonic waveguide made of double chain of silver nanocylinders

The parameters used for the plasmonic waveguide in this example are: the radius of each nanocylinder $r = 50\ nm$, width of $w_P = 300\ nm$, and the distance between the centers of the upper and lower cylinders in the double chain (pitch) $\Lambda = 200\ nm$, while the centre-centre distance of the adjacent cylinders is $120\ nm$ along each chain.

To guide the energy from the focus of the lens to the plasmonic waveguide, similar to Zhan et al. [9], a cone-shaped cylinder array coupler, which consists of nine cylinders, each one has a radius width of $50\ nm$, and the centre-centre distance is $200\ nm$ are used. This cone-shaped coupler has a height of $700\ nm$ which corresponds to about 2.53 of the FWHM ($277\ nm$) of the focus, allowing the energy concentrated in the focus be guided into the plasmonic waveguide. The use of the conical coupler ensures that not only the field that is concentrated in the FWHM, but also the field in the lateral lobes of the focus be coupled to the plasmonic waveguide. In order to have a high coupling efficiency value in the structure, it is necessary that the plasmonic lens chosen, in addition to having a high energy

concentration and a minimum FWHM value at the focus, the coupling distance A must be properly matched.

To find the best distance A between the plasmonic waveguide and the lens, to obtain a good coupling efficiency, in Fig. 12, is calculated the average power density at the center of the transversal domain, $y = 0$, of the plasmonic waveguide in function of the wavelength and the following values of the *A* are conisdered: $600\ nm$ (red line), $826\ nm$ nm (green line), $1000\ nm$ (blue line). For comparison, Fig. 12, also show the average power density without using the plasmonic coupler (black line). The average power density when using plasmonic lens is better than without using lens for wavelengths less than $825\ nm$, $766\ nm$, $743\ nm$ for *A* values $826\ nm$, $600\ nm$ and $1000\ nm$, respectively. These results show that an optimal coupling efficiency can be obtained using plasmonic lenses but for small wavelength ranges. Furthermore, average power density exhibits an approximately linear decay in the entire wavelength domain.
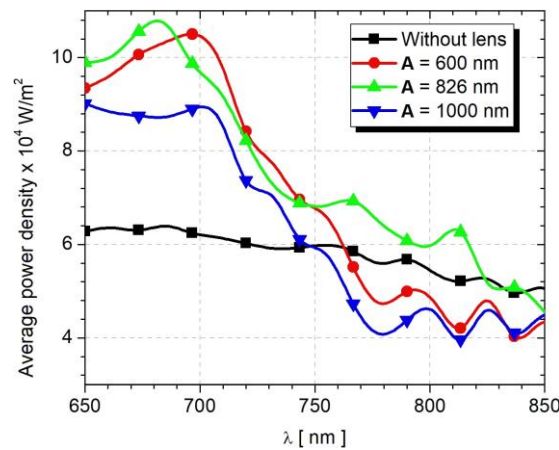

Fig. 12. Average power density at the centre of each pair of cylinders in the double chain axis for a wavelength band from 650 nm to 850 nm. Three different values of the distance between the lens and the plasmonic waveguide, A, are considered: 600 nm, 826 nm and 1000 nm.

In Fig. 13, a comparison between structures without and with plasmonic lens is performed, in which the magnetic field distribution, along the *z* propagation direction, can be observed.
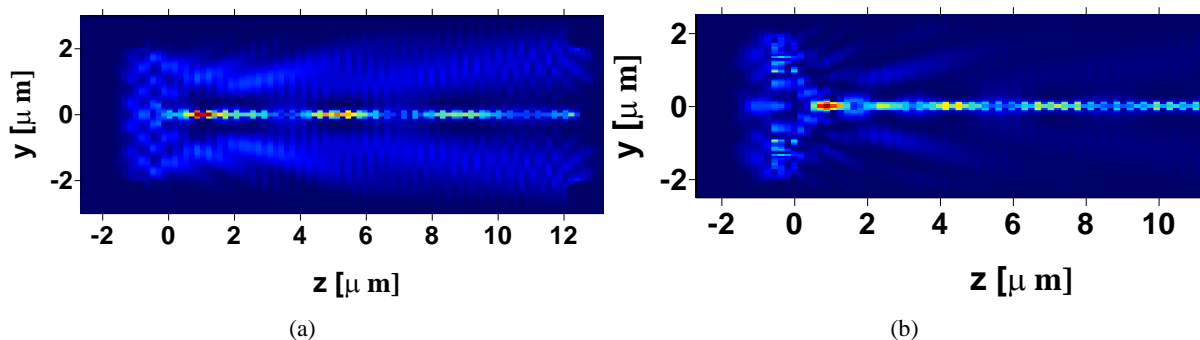

(a)

(b)

Fig. 13. Magnetic field distribution, in the longitudinal section, at $\lambda = 685$ nm for the structure (a) without using the plasmonic lens and (b) using the plasmonic lens coupler with A =826 nm.

Finally, in Fig. 14 the transversal magnetic field intensity is shown at $z = 13.061\ \mu m$ and $\lambda = 685\ nm$. It is possible to observe that with the use of the plasmonic lens there was a significant increase of the field intensity in the core of the waveguide and a reduction on the sides lobes, thus indicating a

small scattering of the light beam along the waveguide and a good concentration of energy in the waveguide core, as shown in Fig. 13(b).
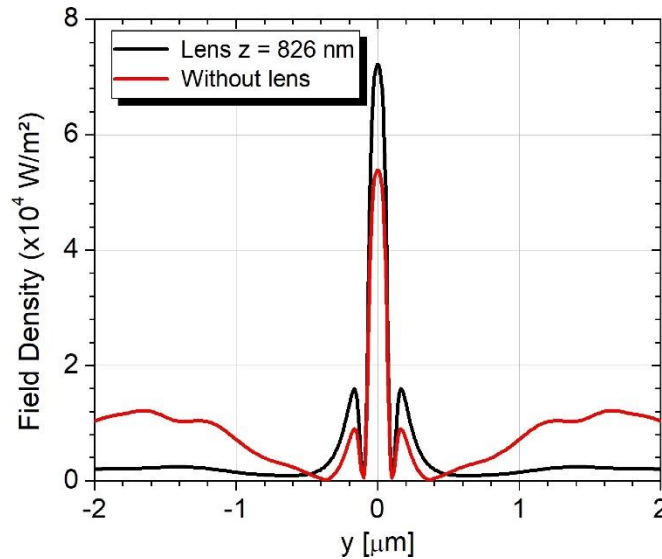

Fig. 14. Transversal magnetic field intensity, **H**z, at z = 13.061 μm and λ = 685 nm for the structure with plasmonic coupler (black line) and without the use on lens (red line).

V. CONCLUSIONS

In this work, an extensive numerical analysis of the propagation of electromagnetic waves in plasmonic structures was carried out, in order, to verify the coupling between a source and waveguides using the 2D-FEM. Initially, the behaviour of plasmonic lenses was studied, in which it was noticed that for silver plasmonic lens with Ag thickness $d = 550\ nm$ and minimum spacing between slits $e = 35\ nm$ at a wavelength of $\lambda = 650\ nm$, called in this work an "optimal plasmonic lens", the best results were obtained in relation to the energy focal depth parameter. Next, the use of these lenses was verified to perform the coupling of a source in two types of plasmonic waveguides to verify their coupling efficiencies. Comparisons of the average power density along the centreline of the plasmonic waveguide with and without use of the lenses as a function of wavelength were performed. An increase in power density was observed for wavelengths smaller than $750\ nm$ when using the plasmonic lens for the coupling. In this context, based on the results obtained numerically, plasmonic lenses have great potential for light coupling in nanophotonic waveguides with dimensions smaller than the operation wavelength.

REFERENCES

[1] H. Shi, C. Wang, C. Du, X. Luo, X. Dong and H. Gao, "Beam manipulating by metallic nano-slits with variant widths," *Opt. Express*, vol. 13, pp. 6815–6820, 2005.

[2] T. Xu, C. Du, C. Wang and X. Luo, "Subwavelength imaging by the metallic slab lens with nanoslits," *Appl. Phys.Lett.*, vol. 91, p. 201501, 2007.

[3] Y. Zhao, S. Lin, A. Nawaz, B. Kiraly, Q. Hao, Y. Liu and T. Huang, "Beam bending via plasmonic lenses," *Opt. Express*,vol. 18, pp. 23 458–23 465, 2010.

[4] N. Engheta, A. Salandrino, and A. Alu, "Circuit elements at optical frequencies: Nanoinductors, nanocapacitors, andnanoresistors," *Physical Review Letters*, vol. 95, p. 095504, 2005.

[5] R. Merlin, "Radiationless electromagnetic interference: Diffractive evanescent-field lenses and perfect focusing," *Science*,vol. 317, pp. 927–929, 2007.

[6] A. Grbic and R. Merlin, "Near-field focusing plates and their design," *IEEE Transaction on Antennas and Propagation*,vol. 56, pp. 3159–3165, 2007.

[7] Y. Jiang, S. Pillai and M. Green, "Realistic silver optical constants for plasmonics," *Scientific Report*, vol. 56, p. 30605,2016.

[8] A. da Silva, *Estudo de uma lente plasmônica para acoplamento em nanoestruturas (Phd. Thesis)*. Faculdade de Engenharia Elétrica - Unicamp, Campinas-SP, 2011.

[9] C. Zhan, X. Ren, H. Huang, K. Duan and G. Guo, "Fdtd studies of metallic cylinder arrays: Plasmons waveguide andy–splitter," *CHIN. PHYS. LETT*, vol. 25, pp. 559–562, 2007.

[10] N. H. O. Cunha and J. P. da Silva, "High Sensitivity Surface Plasmon Resonance Sensor Based on a Ge-Doped Defect and D-Shaped Microstructured Optical Fiber", *Sensors*, vol. 22, pp. 3220, 2022.

[11] X. Chen and H. Ming, "Review of Surface Plasmon Resonance and Localized Surface Plasmon Resonance Sensors", *Photonics Sensors*, vol. 2, pp. 37 – 49, 2012.

[12] D. Paul and R. Biswas, "Influence of Probe Geometry of Optical Fibers in Sensing Volatile Liquids Through Localized Surface Plasmon Resonance", *IEEE Trans. Nanotechnol*, vol. 20, pp. 69 – 74, 2021.

[13] N. H. O. Cunha, *Análise de Células Unitárias Com Metamaterial Utilizando Substratos EBG para Aplicações em Estruturas Planares (M.Sc. Dissertation)*. pp. 3, Programa de Pós-Graduação em Engenharia Elétrica e da Computação – UFRN, Natal – RN, 2020.

[14] V. G. Veselago, "The Electrodynamics of Substances with Simultaneously Negative Values of ε and μ", *Sov. Phys. Uspekhin*, vol. 10, 1968.

[15] J. B. Pendry, "Negative Refraction Makes a Perfect Lens", *Phys. Rev. Lett.*, vol. 85, 2000.

[16] J. H. Choi, J. H Lee, J. Son and J. W. Choi, "Noble Metal-Assisted Surface Plasmon Resonance Immunosensors", *Sensors*, vol. 20, pp. 1003, 2020.

[17] P. K. Jain, X. Huang, I. H. El-Sayed and M. A. El-Sayed, "Noble Metals on the Nanoscale: Optical and Photothermal Proprieties and Some Applications in Imaging, Sensing, Biology, and Medicine", *Acc. Chem. Res.*, vol. 41, pp. 1578 – 1586, 2008.

[18] A. J. Carroll, G. A. van Riessen, E. Balaur, I. P. Dolbnya, G. N. Tran and A. G. Peele, "An iteractive method for near-field Fresnel region polychromatic phase contrast imaging", *Journal of Optics*, vol. 19, 2017.

[19] C. Rubio-Mercedes and H. Hernández-Figueroa, "Padé boundary conditions for the finite-element solution of arbitraryplanar junctions," *J. of Lightwave Technol.*, vol. 22, pp. 669–676, 2004.

[20] Y. Tsuji and M. Koshiba, "Finite Element Method Using Port Truncation by Perfectly Matched Layer Boundary Conditions for Optical Waveguide Discontinuity Problems", *Journal of Lightwave Technol*, Vol. 20, 463-470, (2002).